

# Lattice Dynamics and Electron Pairing in High Temperature Superconductors

A. Lanzara<sup>1,2</sup>, G.-H. Gweon<sup>3</sup>, S. Y. Zhou<sup>1</sup>

<sup>1</sup>*Department of Physics, University of California, Berkeley, CA 94720, U.S.A.*

<sup>2</sup>*Materials Sciences Division, Lawrence Berkeley National Laboratory, Berkeley, CA 94720, U.S.A.*

<sup>3</sup>*Lawrence Berkeley National Laboratory, Berkeley, CA 94720, U.S.A.*

**Abstract:** Angle resolved photoemission spectroscopy combined with isotope substitution ( $^{16}\text{O}\rightarrow^{18}\text{O}$ ) sample preparation method is used to probe the effect of the lattice degrees of freedom on the electron dynamics of optimally doped  $\text{Bi}_2\text{Sr}_2\text{CaC}_2\text{O}_{8+\delta}$  high temperature superconductors, as a function of momentum and temperature. Our data show that the lattice dynamics strongly renormalizes the electron dispersion and the photoemission line shapes. The renormalization is enhanced near the anti-nodal region and in the superconducting state, i.e. as the superconducting gap opens up. This unusual behavior is direct evidence that the electron-phonon interaction is correlated with the electron pairing in the high temperature superconductivity.

**Key words:** High Temperature Superconductors, ARPES, coherent quasiparticle, incoherent quasiparticle, isotope substitution.

One of the ongoing debates in the field of high temperature superconductors is whether the lattice degrees of freedom are responsible for some of the unusual electronic properties of the cuprates. While many experiments have pointed out that the lattice is heavily involved in several properties of the cuprate superconductors [1], the lack of experiments probing directly the electronic response to the lattice has kept the debate open. In addition, the absence of a pronounced conventional isotope effect [2] on the critical temperature ( $T_c$ ) [3, 4], has reinforced the belief that the magnetic interaction is the main player instead. However, the meaning of this small isotope coefficient of  $T_c$  is unclear since even for conventional superconductors screening can induce small and/or negative value of the isotope coefficient [5]. Indeed, there are several experiments suggesting the presence of a strong electron-phonon interaction in the cuprates, for example the observation of a phonon “kink” in the quasiparticle dispersion measured by photoemission spectroscopy [6], the presence of a very large isotope effect on the pseudogap formation temperature [7,8] and the magnetic susceptibility [9], and the observation of an anomalous isotope effect on the in-plane far-infrared optical conductivity [10].

Here we report the first experimental results where the electronic response to the lattice degrees of freedom is directly measured. This is made possible by combining angle resolved photoemission spectroscopy (ARPES) and oxygen isotope substitution on high temperature superconductors.

ARPES data were collected at beamline 10.0.1 of the Advance Light Source using a SCIENTA 2000 analyzer on optimally doped oxygen isotope substituted  $\text{Bi}_2\text{Sr}_2\text{CaC}_2\text{O}_{8+\delta}$  (Bi2212) ( $T_c=92\text{K}$ ) superconductors. Upon isotope substitution ( $^{16}\text{O}\rightarrow^{18}\text{O}$ ),  $T_c$  changes to 91K. The details of isotope substitution are described elsewhere [11]. The energy resolution was of 15 meV FWHM and the angular resolution of 0.15 degree, corresponding to momentum resolution better than 0.01 p/a. The vacuum during the

measurement was better than  $5 \times 10^{-11}$  Torr. The photon energy was 33 eV. Data were collected for scans parallel to the nodal cut  $\Gamma Y$ , (0, 0) to ( $\pi$ ,  $\pi$ ), of the Brillouin zone, at two different temperatures, below (25K) and above (100K)  $T_c$ . Each cut is assigned a cut number, which is the angle offset from the nodal direction. For example, cut 0 will mean a nodal cut, and cut 6 will mean a cut 6 degrees displaced from the nodal cut.

In Figure 1 we show the raw ARPES data as image plots, for several cuts in the momentum space, from the nodal  $\Gamma Y$  (panel a0 and b0) to half way towards the M point ( $\pi$ , 0) (panels a6 and b6), for the two isotope substituted samples. The color scale represents the photoelectron intensity versus the momentum and binding energy, with maximum in black and minimum in white. The reversibility of the isotope effect upon the isotope re-substitution ( $^{18}\text{O} \rightarrow ^{16}\text{O}$ ) has been shown elsewhere [11].

The intensity maps shown in Figure 1 were normalized (i.e. shifted and scaled in intensity) in such a way that each energy distribution curve (EDC) at each momentum value has intensity range from 0 to 1. This new way of presenting the data allows an easy overview of main differences between the two isotopes, because the information regarding the energy-momentum dispersion relation and the line widths can be already “read off” from the images, without actually applying EDC fit procedures, which are not so straightforward in general. Because of this reason, we will refer to these maps as “pro-EDC maps.”

In particular, the maps in Figure 1 make it very easy to see the dichotomy of two dispersing branches, sharp low energy branch (sharp peaks) and broad high-energy branch (broad humps). Note that throughout this paper we use the terms energy and binding energy interchangeably. Following the Fermi liquid terminology, we refer to the low energy branch as coherent branch, while we refer to the high-energy branch as incoherent branch. Also, we will loosely refer to the sharp peak near Fermi level ( $E_F$ ; defined as zero throughout the paper) as “coherent quasi-particle” peak.

In these pro-EDC maps, the kink phenomenon [6] is visualized as the crossover from the low energy quasi-particle branch to the high-energy incoherent branch. This crossover region is the region of low intensity (indicated by white dashed line, and blue and red arrows), where the two dispersions mix and give rise to a double peak structure, commonly referred to as a “peak-dip-hump” structure, of EDC’s [6,12-14]. In this terminology, the dip energy corresponds to the kink energy, and coincides with the position of the dispersion kink, i.e. change of velocity, in momentum distribution curve (MDC) analysis [15].

Another feature to note in Figure 1 is the superconducting gap, which increases as we approach the antinodal point (from cut 0 to cut 6). The isotope dependence of the gap was discussed in details in Ref.’s [11,16]. Note that in pro-EDC maps, the apparent gap, i.e. the closest approach of the low energy branch to the Fermi level, is often given by the instrumental energy resolution, which is the case for near-nodal cuts in Figure 1. This is of course not the true gap. However, when the true gap value becomes bigger than the energy resolution, the peak position is a good representation of the gap, as for cuts 5-6. For smaller gaps, MDC analysis, presented before [11], is essential.

We will now focus on the differences between the two isotope samples. As is well known in band theory [17], the total energy range of the dispersion decreases as we move towards the antinodal point (cut 6). Upon a close inspection of the images (see also white dotted lines extracted from EDC peak position), we find that the most striking change induced by the isotope substitution occurs at high energy and is manifested by a reduction of the binding energy of the incoherent branch, all the way up to the highest energy shown (see black arrows in panels a and b). On the contrary, the low energy dispersion is weakly isotope dependent, similar to its weak doping dependence [18].

This isotope dependence is strongly momentum dependent. As we move from the nodal (panels a0, b0) to the antinodal region (panels a6,b6), comparison between the upper ( $^{16}\text{O}$  data) and the lower ( $^{18}\text{O}$  data) panels clearly shows that the isotope-induced changes are enhanced closer to the antinodal region (cuts 5,6). More specifically we see that the isotope substitution induces a narrowing of the band width up to 20%, near the antinodal region (compare panel a6 to b6), by a factor of two bigger, in absolute energy, than along the nodal direction [11]. We note that the shift of the incoherent peak in the EDC's cannot be accounted for by a rigid shift due to the isotope-induced change of the superconducting gap, which decreases only by few meV upon isotope substitution, as can be seen from the change in the leading edge position.

Another important observation is that, in addition to the isotope-induced change in the band width, there is a clear isotope-induced narrowing of the EDC's [16], as can be noticed by the broader black shadowed area for  $^{16}\text{O}$  sample (upper panels), with respect to the  $^{18}\text{O}$  sample (lower panels). The width changes become appreciable only in the incoherent part of the dispersion. Again the changes are maximum near the antinodal region. Panel c shows an explicit comparison of the EDC's where the EDC narrowing of the  $^{18}\text{O}$  sample can be clearly noted.

Figure 1 summarizes our main findings: a) the isotope substitution strongly affect the high energy incoherent quasiparticle spectra, inducing a reduction of the bandwidth and a narrowing of the line shape width upon  $^{18}\text{O}$  substitution, b) The isotope effect is energy dependent: i.e. it is negligible at low energy scale and is strongly enhanced at high energy; c) the kink energy separates the low energy region where the isotope effect is negligible from the high energy region where the effect is strong, thus putting a strong constraint on the phonon involvement in the kink dynamics.

In Figure 2 we report raw normal state (100K) ARPES data for similar cuts as in figure 1. The most striking observation from the data is the similarity between the  $^{16}\text{O}$  and  $^{18}\text{O}$  data, (compare upper and lower panels). The reduction of the isotope effect can be also seen from the EDC peaks (panel c). No appreciable change of the peak position or peak width is observed at this high temperature. The reduction of the isotope effect in the normal state suggests that the low temperature behavior is associated with the onset of additional scattering mechanism. This unusual temperature dependence is also consistent with other experimental results where an enhancement of the isotope effect is observed below  $T^*$ . The onset of electron-phonon interaction in the superconducting state is unusual in term of conventional electron-phonon interaction where one would expect that the phonon contribution is weakly dependent on the temperature [19], and

*increase* at high  $T$ . Indeed, based on this naive expectation, this type of unconventional  $T$  dependence has been often used to *rule out* phonons. Here, however, we see clearly that this reasoning is not justified. Moreover, this type of unconventional enhancement of the electron phonon interaction below a characteristic temperature scale is actually expected for other systems such as spin-Peierls systems or charge density wave (CDW) systems. Thus, our results put an important constraint on the nature of the electron phonon interaction in these systems.

In Figure 3 we report a quantitative comparison of the isotopes-induced changes in peak positions and line shapes. Panel a shows the momentum dependence of the high-energy isotope-induced changes of the EDC peak positions, plotted as a function of the superconducting energy gap ( $\Delta$ ). Clearly the isotope induced changes increase as the antinodal direction is approached, consistent with the observations made above with Figures 1 and 2. Additionally there is a strong correlation of the isotope-induced change of the dispersion with the momentum dependence of the superconducting gap [11]. This observation strongly suggests that the high-energy states are correlated with the superconducting transition.

In panels b1 and b2 we show the difference of the EDC widths between the two isotopes, as a function of energy (peak position), for the nodal and antinodal cuts respectively (cuts 0 and 6). The difference is taken in the superconducting state. For the measure of the width, the FWHM on the low energy side is used since the FWHM on the high-energy side is difficult to extract due to the strong high-energy intensity tail. We observe that the isotope-induced changes in both cases turn on gradually above  $\sim 60\text{meV}$ , which corresponds to the kink position. This effect may already be observed qualitatively in Figure 1, and coincides with the other two phenomena discussed with that figure, namely sudden broadening of EDC peak and sudden increase of the isotope effect of EDC dispersion as energy increases beyond the kink energy. Clearly the effect is stronger in the antinodal direction (panel b2) where the total isotope-induced narrowing of the peak width is by a factor of two bigger than for the nodal direction. To study the details of the momentum dependence of the incoherent peak width upon isotope substitution, in panel c we report FWHM of the high-energy isotope-induced changes versus superconducting gap. The overall trend is an increase of the effect as the antinodal is approached (large gap). On the other hand, in the low energy part, the isotope dependence of the width is negligible and slightly dependent of the momentum (i.e. superconducting gap). There are two major important observations from these analyses. The first is that there is overall a narrowing of the peak width upon isotope substitution. Such narrowing could be due to multi-phonon contribution [11]. In addition the narrowing of the peak becomes stronger as we approach the antinode. This result clearly suggests that low energy quasi-particles are more heavily dressed in the superconducting state and near the anti-nodal region. The strong isotope dependence means that phonons are an important part of this dressing.

In conclusion our data clearly point to a picture where the electron dynamics is strongly renormalized by interaction with the lattice. Further, this renormalization has a strong correlation with the superconducting gap, since it is large in the anti-nodal region and at low temperature. In terms of energy dependence, the renormalization of the quasiparticle dynamics is

strongest in the energy window of  $J$  to  $2J$ , where  $J$  is the anti-ferromagnetic exchange interaction, and is reduced for larger energies [11]. Thus, the energy region where phonons are active coincides with the energy region dominated by the strong electron correlation. This is strongly suggestive that there is a cooperative interplay between the two degrees of freedom, lattice and spin. Specifically, we have proposed [11] that the dynamic spin-Peierls physics [20] summarizes the essence of our results, and is responsible for the enhanced electron-phonon interaction at low temperature.

In view of this scenario, it is expected that the exchange interaction  $J$  is affected by the isotope substitution.

*Acknowledgement:* We would like to thank Dung-Hai Lee for useful discussions. H. Takagi and T. Sasagawa for providing us with high quality oxygen isotope substituted single crystals and J. Graf for experimental help.

### References:

- [1] Review phonons
- [2] Maxwell, E. Isotope Effect in the Superconductivity of Mercury. *Phys. Rev.* **78**, 477 (1950)
- [3] Crawford, M. K. *et al.* Oxygen Isotope Effect and Structural Phase Transitions in  $\text{La}_2\text{CuO}_4$ -Based Superconductors. *Science* **250**, 1390 (1990)
- [4] For a review see J. P. Franck in *Physical Properties of High Temperature Superconductivity IV*, edited by D. S. Ginsberg (World Scientific Singapore, 1994).
- [5] Isotope unconventional
- [6] Lanzara, A., P. V. Bogdanov, X. J. Zhou, S. A. Kellar, D. L. Feng, E. D. Lu, T. Yoshida, H. Eisaki, A. Fujimori, K. Kishio, J. I. Shimoyama, T. Noda, S. Uchida, Z. Hussain, Z. X. Shen, Evidence for ubiquitous strong electron-phonon coupling in high-temperature superconductors. *Nature* **412**, 510-514 (2001)
- [7] Lanzara, A. *et al.* Oxygen-isotope Shift of the Charge-Stripe Ordering Temperature in  $\text{La}_{2-x}\text{Sr}_x\text{CuO}_4$  from X-ray Absorption Spectroscopy, *J. Phys. Condens. Mat.* **11**, L541-L544 (1999)
- [8] D. R. Temprano *et al.* *Phys. Rev. Lett.* **84**, 1990 (2000)
- [9] Zhao, G. M., Keller H., and Conder, K. Unconventional Isotope Effect in the High-Temperature Cuprate Superconductors. *J. Phys. Condens. Mat.* **13**, R569 (2001) and references therein.
- [10] C. Bernhard, T. Holden, A. V. Boris, N. N. Kovaleva, A. V. Pimenov, J. Humlicek, C. Ulrich, C. T. Lin and J. L. Tallon, Anomalous oxygen-isotope effect on the in-plane far-infrared of detwinned  $\text{YBa}_2\text{Cu}_3^{16,18}\text{O}_{6,9}$  *Phys. Rev. Lett.* **69**, 052502 (2004)
- [11] G. H. Gweon, T. Sasagawa, S. Y. Zhou, J. Graf, H. Takagi, D. H. Lee and A. Lanzara. *To be published Nature* (2004)
- [12] Dessau, D. S. *et al.* Anomalous spectral weight transfer at the superconducting transition of  $\text{Bi}_2\text{Sr}_2\text{CaCu}_2\text{O}_{8+\delta}$ . *Phys. Rev. Lett.* **66**, 2160-2163 (1991)
- [13] Shen, Z.-X. and Schrieffer, J. R., Momentum, Temperature, and Doping Dependence of Photoemission Lineshape and Implications for the Nature of the Pairing Potential in High- $T_c$  Superconducting Materials. *Phys. Rev. Lett.* **78**, 1771-1774 (1997)
- [14] Norman, M. R. *et al.* Unusual Dispersion and Line Shape of the Superconducting State Spectra of  $\text{Bi}_2\text{Sr}_2\text{CaCu}_2\text{O}_{8+\delta}$ . *Phys. Rev. Lett.* **79**, 3506-3509 (1997)
- [15] Bogdanov, P. V. , A. Lanzara, S. A. Kellar, X. J. Zhou, E. D. Lu, W. J. Zheng, G. Gu, J. I. Shimoyama, K. Kishio, H. Ikeda, R. Yoshizaki, Z. Hussain and Z. X. Shen, Evidence for an energy scale for quasiparticle dispersion in  $\text{Bi}_2\text{Sr}_2\text{CaCu}_2\text{O}_8$ . *Phys. Rev. Lett.* **85**, 2581-2584 (2000)

- [16] G.-H. Gweon, S. Y. Zhou, J. Graf, T. Sasagawa, H. Takagi, A. Lanzara in preparation
- [17] Norman, M. R., Randeria, M., Ding, H., and Campuzano, J. C. Phenomenological models for the gap anisotropy of  $\text{Bi}_2\text{Sr}_2\text{CaCu}_2\text{O}_8$  as measured by angle-resolved photoemission spectroscopy. *Phys. Rev. B* **52**, 615-622 (1995)
- [18] Zhou, X. J. *et al.* Universal Nodal Fermi Velocity. *Nature* **423**, 398 (2003)
- [19] Scalapino, D. J. in *Superconductivity* (ed. Parks, R. D.) 449 (Marcel Dekker, New York, 1969)
- [20] Pytte, E. Peierls instability in Heisenberg chains. *Phys. Rev. B* **10**, 4637-4642 (1974)

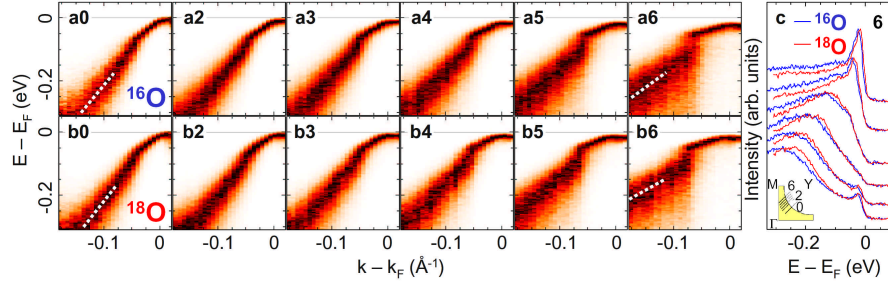


**Fig. 1** Low temperature (25 K) ARPES data of optimally doped  $\text{Bi}_2\text{Sr}_2\text{CaC}_2\text{O}_{8+\delta}$  high temperature superconductors with oxygen isotope  $^{16}\text{O}$  (panels a) and  $^{18}\text{O}$  (panels b). These maps are normalized so that the intensity of each EDC goes from 0 to 1 (see text for details). The panels are labelled with a cut number, i.e. angle offset from the nodal cut. Inset of panel c shows the cut numbers. In panel c, isotope dependence of a few selected EDC's are shown for cut 6. The top pair corresponds to  $k=k_F$ , i.e. momentum value on the normal state Fermi surface, shown as a curve in the inset.

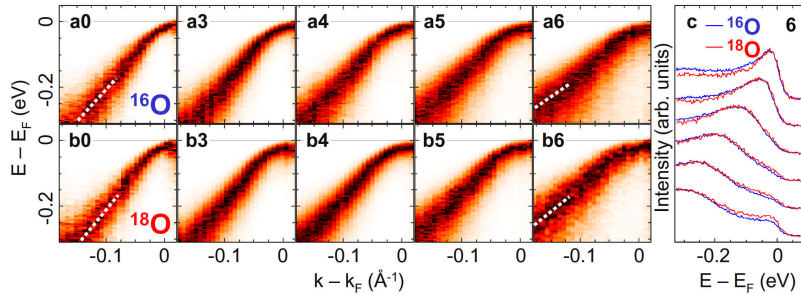


**Fig. 2** Same as Fig. 1, except for the high measurement temperature (100 K).

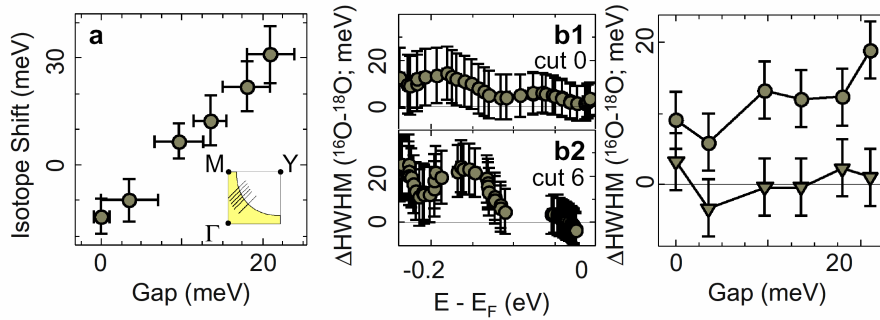


**Fig. 3** (a) The isotope shift of the high energy EDC vs. the superconducting gap ( $\Delta$ ), for the 6 cuts shown in Fig. 1. The isotope shift is measured at the same energy (220 meV, isotope average) for all cuts. The superconducting gap is the average value between the two isotope samples. (b) The isotope difference of the EDC widths for cuts 0 and 6. The width is measured in HWHM, on the low energy side of each EDC, i.e. between the peak position and the Fermi energy. The horizontal axis corresponds to the peak position at which the isotope difference of the width was extracted. (c) Isotope difference for each cut, averaged and plotted as a function of the isotope-averaged superconducting gap. HE (circles) refers to average over high energy (-220 meV to -70 meV) and LE (triangles) refers to average over low energy (-70 meV to 0).